

A coupled spin-electron diamond chain with different Landé g-factors of localized Ising spins and mobile electrons

Jordana Torrico¹, Maria Socorro Seixas Pereira¹, Jozef Strečka², Marcelo Leite Lyra¹

¹*Instituto de Física, Universidade Federal de Alagoas, 57072-970 Maceió, Alagoas, Brazil and*

²*Department of Theoretical Physics and Astrophysics, Faculty of Science, P. J. Šafárik University, Park Angelinum 9, 040 01 Košice, Slovakia*

A coupled spin-electron diamond chain with localized Ising spins placed on its nodal sites and mobile electrons delocalized over interstitial sites is explored in a magnetic field taking into account the difference between Landé g-factors of the localized spins and mobile electrons. The ground-state phase diagram is constituted by two classical ferrimagnetic phases, the quantum unsaturated paramagnetic phase and the saturated paramagnetic phase. Both classical ferrimagnetic phases as well as the unsaturated paramagnetic phase are reflected in a low-temperature magnetization curve as intermediate magnetization plateaus. The unsaturated paramagnetic phase is quantum in its character as evidenced by the fermionic concurrence calculated for a pair of the mobile electrons hopping in between the interstitial sites. It is shown that the magnetic field can under certain conditions induce a quantum entanglement above the disentangled ground state.

PACS numbers: 05.50.+q, 75.10.Pq, 75.30.Kz, 75.40.Cx

I. INTRODUCTION

Frustrated spin systems exhibit a variety of exotic quantum ground states, which may provide an interesting alternative for a quantum information processing [1]. The geometric spin frustration is most commonly introduced through competing antiferromagnetic interactions between the localized spins situated on non-bipartite lattices. Another remarkable alternative represents a kinetically-driven spin frustration of the localized spins, which is invoked by a quantum-mechanical hopping process of the mobile electrons. The latter type of spin frustration has been found for instance in the coupled spin-electron diamond chain [2–5]. Last but not least, recent studies motivated by a magnetic behavior of the copper-iridium oxides have revealed another peculiar mechanism of the spin frustration, which originates from a non-uniformity of the Landé g-factor [6].

In the present work, we will explore a combined effect of the kinetically-driven spin frustration and the spin frustration stemming from the non-uniformity of the Landé g-factors by generalizing the exact solution for the coupled spin-electron diamond chain [2–5]. Following the procedure elaborated in our previous work [5] we will compute the fermionic concurrence between the pair of mobile electrons in order to demonstrate how the magnetic field may induce a quantum entanglement above the disentangled zero-field ground state.

II. MODEL AND METHOD

Let us consider a coupled spin-electron diamond chain, which is composed of the localized Ising spins situated on its nodal lattice sites and two mobile electrons hopping on the pairs of interstitial sites (see Fig. 1 of Ref. [5] for illustration). The total Hamiltonian of the model

under investigation can be written as a sum of the cell Hamiltonians $\mathcal{H} = \sum_i \mathcal{H}_i$, whereas each cell Hamiltonian \mathcal{H}_i involves all the interaction terms belonging to the i -th diamond unit:

$$\begin{aligned} \mathcal{H}_i = & -t \sum_{\gamma=\uparrow,\downarrow} \left(c_{i1,\gamma}^\dagger c_{i2,\gamma} + \text{h.c.} \right) - g_1 h \sum_{j=1}^2 (n_{ij,\uparrow} - n_{ij,\downarrow}) \\ & + J (\sigma_i + \sigma_{i+1}) \sum_{j=1}^2 (n_{ij,\uparrow} - n_{ij,\downarrow}) - g_2 \frac{h}{2} (\sigma_i + \sigma_{i+1}). \end{aligned} \quad (1)$$

Here, $c_{i\alpha,\gamma}^\dagger$ and $c_{i\alpha,\gamma}$ are fermionic creation and annihilation operators for an electron with the spin $\gamma = \uparrow, \downarrow$ hopping on the pairs of interstitial sites $\alpha = 1, 2$, $n_{i\alpha,\gamma} = c_{i\alpha,\gamma}^\dagger c_{i\alpha,\gamma}$ is respective number operator. The parameter t is the hopping term associated with the kinetic energy of the mobile electrons, the coupling constant J stands for the Ising interaction between the nearest-neighbor localized spins and mobile electrons, h is the external magnetic field accounting for the difference between the Landé g-factors g_1 and g_2 of the mobile electrons and localized Ising spins, respectively (Bohr magneton μ_B was absorbed into a definition of the field term h).

An exact solution for the coupled spin-electron diamond chain can be straightforwardly obtained by adapting the procedure reported in our previous work [5] by a mere replacement of the uniform magnetic field h through two different local magnetic fields $g_1 h$ and $g_2 h$. The readers interested in details of the calculation procedure are therefore referred to Ref. [5].

III. RESULTS AND DISCUSSION

Let us proceed to a discussion of the most interesting results for the coupled spin-electron diamond chain with

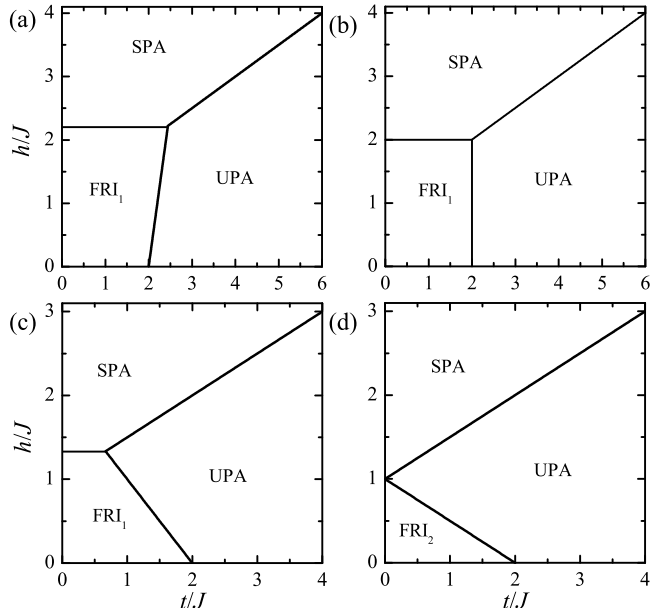


Figure 1: The ground-states phase diagram in the t/J - h/J plane for the fixed value of the Landé g -factor of the mobile electrons $g_1 = 2$ and a few different values of the Landé g -factor of the localized Ising spins: (a) $g_2 = 1.8$; (b) $g_2 = 2$; (c) $g_2 = 3$; (d) $g_2 > 4$.

the antiferromagnetic exchange interaction $J > 0$, which exhibits the most outstanding magnetic features due to a spin-frustration effect. For simplicity, our further attention will be restricted to the most common special case with the fixed value of the Landé g -factor of the mobile electrons $g_1 = 2$, whereas an influence of the Landé g -factor of the localized Ising spins on the overall magnetic behavior will be subject of our investigations.

A. Ground-state phase diagram

The ground-state phase diagram (Fig. 1) involves two ferrimagnetic phases (FRI₁ and FRI₂), the unsaturated paramagnetic phase (UPA) and the saturated paramagnetic phase (SPA) given by the eigenvectors:

$$|\text{FRI}_1\rangle = \prod_{i=1}^N |\downarrow\rangle_{\sigma_i} \otimes |\uparrow, \uparrow\rangle_i \quad (2)$$

$$|\text{FRI}_2\rangle = \prod_{i=1}^N |\uparrow\rangle_{\sigma_i} \otimes |\downarrow, \downarrow\rangle_i \quad (3)$$

$$|\text{UPA}\rangle = \prod_{i=1}^N |\uparrow\rangle_{\sigma_i} \otimes \frac{1}{\sqrt{2}} [|\uparrow, \downarrow\rangle_i + |\downarrow, \uparrow\rangle_i - |\uparrow, 0\rangle_i - |0, \uparrow\rangle_i] \quad (4)$$

$$|\text{SPA}\rangle = \prod_{i=1}^N |\uparrow\rangle_{\sigma_i} \otimes |\uparrow, \uparrow\rangle_i. \quad (5)$$

In above, the first ket vector determines the spin state of localized Ising spins and the second one the spin state of the mobile electrons. All magnetic moments of the localized Ising spins and mobile electrons are fully aligned into the magnetic field within the SPA ground state. Owing to the antiferromagnetic interaction $J > 0$, the localized Ising spins tend in opposite to the magnetic field within the FRI₁ ground state and the mobile electrons tend in opposite to the magnetic field within the FRI₂ ground state. However, the most interesting spin arrangement can be found within the UPA ground state, where the hopping process of two mobile electrons with opposite spins leads to a kinetically-driven spin frustration of the localized Ising spins. As a result, the localized Ising spins are polarized by arbitrary but non-zero magnetic field, while the mobile electrons underlie a quantum entanglement of two antiferromagnetic and two ionic states. Note furthermore that the FRI₁ (FRI₂) phase appears in the ground-state phase diagram if $g_2 < 4$ ($g_2 > 4$), while both ferrimagnetic phases coexist together when $g_2 = 4$.

B. Magnetization curves

To get a deeper insight, the total magnetization is plotted in Fig. 2 against the magnetic field together with the sublattice magnetization of the Ising spins and the mobile electrons. The magnetization dependences shown in the first column give evidence for the following sequence of the phase transitions FRI₁-UPA-SPA driven by the rising magnetic field. Contrary to this, the total and sublattice magnetizations plotted in the second column give proof for another sequence of the field-induced phase transitions FRI₂-UPA-SPA. The displayed magnetization curves thus independently verify correctness of the established ground-state phase diagram.

C. Fermionic concurrence

The fermionic concurrence C , which may serve as a measure of bipartite entanglement between two mobile electrons from the same couple of interstitial sites, can be calculated at zero as well as nonzero temperatures according to the procedure described in Ref. [5]. The classical character of the FRI₁, FRI₂ and SPA ground states is consistent with zero concurrence $C = 0$, while its maximum value $C = 1$ reveals a full quantum entanglement within the UPA ground state. Typical thermal dependences of the concurrence are illustrated in Fig. 3. In general, the concurrence monotonically decreases from its maximum value $C = 1$ with increasing temperature when the interaction parameters drive the investigated system towards the UPA ground state. In addition, the concurrence exhibits a more striking non-monotonous thermal dependence if the magnetic field drives the investigated system sufficiently close to a phase boundary between the UPA ground state and one of three classical (FRI₁,

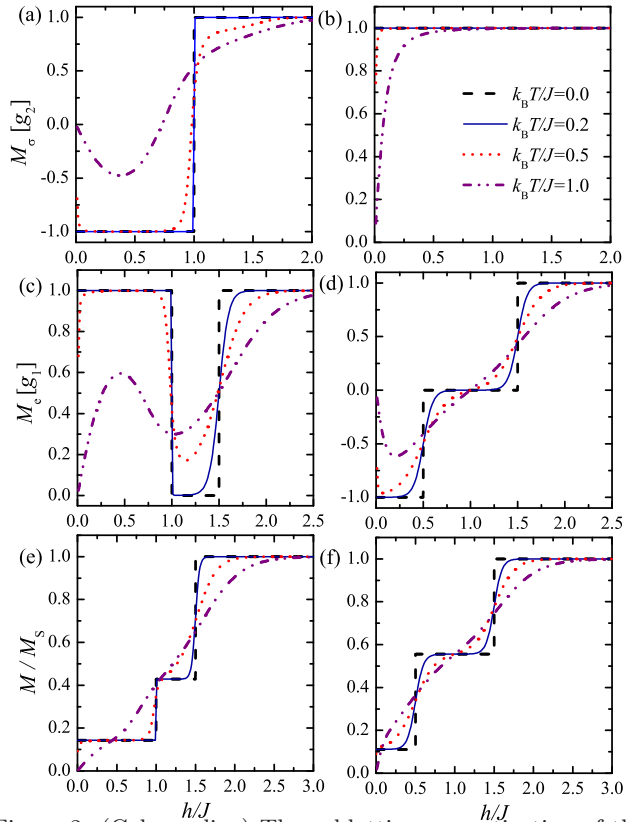


Figure 2: (Color online) The sublattice magnetization of the Ising spins M_σ , the sublattice magnetization of the mobile electrons M_e and the total magnetization as a function of magnetic field for $t/J = 1$, $g_1 = 2$ and a few different values of temperature. The first column corresponds to $g_2 = 3$ and the second column to $g_2 > 4$.

FRI₂ and SPA) ground states. Under this condition, the concurrence shows a peculiar reentrant behavior due to a thermally-induced activation of the UPA spin arrangement, which represents low-lying excited state above one of three classical (FRI₁, FRI₂ and SPA) ground states.

IV. CONCLUSION

In the present work, we have generalized an exact solution for a coupled spin-electron diamond chain by accounting for a difference between the Landé g -factors of the localized Ising spins and mobile electrons. The ground-state phase diagram, magnetization process and

fermionic concurrence have been investigated in particular. It has been verified that the ground-state phase diagram involves two classical ferrimagnetic phases FRI₁ and FRI₂, the quantum unsaturated paramagnetic phase UPA as well as the saturated paramagnetic phase SPA. The ground states FRI₁, FRI₂ and UPA manifest themselves in a low-temperature magnetization curve as intermediate magnetization plateaus. The quantum character of the UPA ground state has been evidenced through the fermionic concurrence, which displays monotonous de-

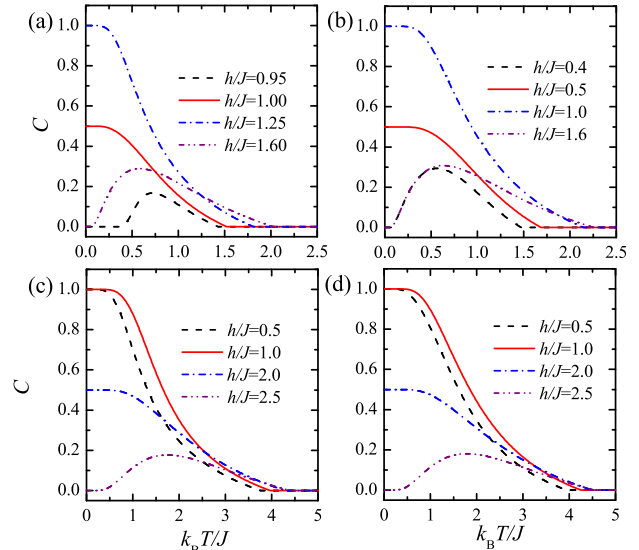


Figure 3: (Color online) Thermal variations of the concurrence at a few different magnetic fields when $g_1 = 2$ is fixed and: (a) $t/J = 1$, $g_2 = 3$; (b) $t/J = 1$, $g_2 > 4$; (c) $t/J = 2$, $g_2 = 3$; (d) $t/J = 2$, $g_2 > 4$.

cline upon rising temperature. It has been also demonstrated that the nonzero fermionic concurrence can be induced above the classical ground states once the magnetic field drives the investigated system sufficiently close to a phase boundary with the UPA ground state.

Acknowledgments

This work was supported by Brazilian agencies FAPEAL, CNPq, CAPES and by Slovak Research and Development Agency under contract No. APVV-0097-12.

-
- [1] M.A. Nielsen, I.L. Chuang, *Quantum Computation and Quantum Information* DOI:10.1080/00107514.2011.587535, Cambridge University Press, Cambridge, 2000.
 [2] M.S.S. Pereira, F.A.B.F. de Moura, M.L. Lyra, *Phys. Rev. B* **77**, 024402 (2008). DOI:10.1103/PhysRevB.77.024402
 [3] M.S.S. Pereira, F.A.B.F. de Moura, M.L. Lyra, *Phys. Rev.*

- B* **79**, 054427 (2009). DOI:10.1103/PhysRevB.79.054427
 [4] B.M. Lisnii, *Low Temp. Phys.* **37**, 296 (2011). DOI:10.1063/1.3592221
 [5] J. Torrico, M. Rojas, M.S.S. Pereira, J. Strečka, M.L. Lyra, *Phys. Rev. B* **93**, 014428 (2016). DOI:10.1103/PhysRevB.93.014428
 [6] W.-G. Yin, Ch.R. Roth, A.M. Tsvetlik, arXiv: 1510.00030.